Nucleoside Diphosphate Kinase B Knock-out Mice Have Impaired Activation of the K$^+$ Channel KCa3.1, Resulting in Defective T Cell Activation

Lie Di[‡1], **Shekhar Srivastava**[‡§1], **Olga Zhdanova**[‡§], **Yi Sun**[‡], **Zhai Li**[‡], and **Edward Y. Skolnik**[‡§2]

From [§]*The Helen L. and Martin S. Kimmel Center for Biology and Medicine at the Skirball Institute for Biomolecular Medicine, Division of Nephrology, and the* [‡]*Departments of Internal Medicine and Pharmacology, New York University Langone Medical Center, New York, New York 10016*

Nucleoside diphosphate kinases (NDPKs) are encoded by the *Nme* (non-metastatic cell) gene family. Although they comprise a family of 10 genes, NDPK-A and -B are ubiquitously expressed and account for most of the NDPK activity. We previously showed that NDPK-B activates the K$^+$ channel KCa3.1 via histidine phosphorylation of the C terminus of KCa3.1, which is required for T cell receptor-stimulated Ca^{2+} flux and proliferation of activated naive human CD4 T cells. We now report the phenotype of *NDPK-B$^{-/-}$* mice. *NDPK-B$^{-/-}$* mice are phenotypically normal at birth with a normal life span. Although T and B cell development is normal in *NDPK-B$^{-/-}$* mice, KCa3.1 channel activity and cytokine production are markedly defective in T helper 1 (Th1) and Th2 cells, whereas Th17 function is normal. These findings phenocopy studies in the same cells isolated from *KCa3.1$^{-/-}$* mice and thereby support genetically that NDPK-B functions upstream of KCa3.1. NDPK-A and -B have been linked to an astonishing array of disparate cellular and biochemical functions, few of which have been confirmed *in vivo* in physiological relevant systems. *NDPK-B$^{-/-}$* mice will be an essential tool with which to definitively address the biological functions of NDPK-B. Our finding that NDPK-B is required for activation of Th1 and Th2 CD4 T cells, together with the normal overall phenotype of *NDPK-B$^{-/-}$* mice, suggests that specific pharmacological inhibitors of NDPK-B may provide new opportunities to treat Th1- and Th2-mediated autoimmune diseases.

Nucleoside diphosphate kinases (NDPKs)[3] are encoded by the *Nme* (non-metastatic cell) genes and comprise a family of 10 related genes that arose by gene duplication (1, 2). Although early studies of the NDPK family were related to their role in the transfer of the γ-phosphate of NTPs to NDPKs via a phosphohistidine intermediate, it is now evident that NDPKs play crucial roles in the regulation of a wide variety of cellular processes (2–4). The *Nme* gene family can be divided into two broad groups based on sequence characteristics and NDPK-A activity (1, 2). Of the group 1 NDPKs, *NDPK-A* and *NDPK-B* (also known as *NM23-H1* and *NM23-H2*) are ubiquitously expressed and account for > 95% of NDPK activity in most cells.

Despite being small proteins of 152 amino acids, NDPK-A and -B have been linked to a wide variety of cellular and biochemical functions. In general, NDPK-A and -B regulate cellular processes via their ability to form multimeric complexes with numerous intracellular targets, leading to the subsequent modulation of their activities via the generation of NTPs, via histidine phosphorylation, via direct protein-protein interaction, or via regulation of downstream signaling pathways (5–12). In addition, NDPKs have been shown to bind DNA, to function as transcriptional activators, and to possess DNase and 3′-5′ exonuclease activity (13, 14).

Although NDPK-A and -B share 88% sequence identity at the protein level, each has been linked to specific biological functions. NDPK-A was first identified as an *in vivo* inhibitor of the metastatic spread of tumors (15–17). NDPK-B, but not NDPK-A, has been shown to play a critical role in T cell receptor (TCR)-stimulated Ca^{2+} influx and activation via its interaction with and activation of the K$^+$ channel KCa3.1 (18). Activation of KCa3.1 plays an important role in T lymphocyte Ca^{2+} signaling by helping to maintain a negative membrane potential, which provides an electrochemical gradient to drive TCR-stimulated Ca^{2+} influx (19, 20). NDPK-B has also been shown to form a complex with the β subunit of G proteins and to participate in G protein activation (6, 21). Knockdown of *NDPK-B*, but not *NDPK-A*, in zebrafish leads to a decrease in cardiac contractility due to down-regulation and mislocalization of heterotrimeric G proteins (22).

Currently, NDPKs are the only known histidine kinases in mammals (8). With regard to activation of KCa3.1, NDPK-B has been shown to phosphorylate the C terminus of KCa3.1 on histidine 358, leading to KCa3.1 activation (18). NDPK-B has also been shown to phosphorylate Gβ at histidine 266. The high energy phosphohistidine intermediate is then transferred to GDP, leading to the generation of GTP and the activation of Gα (6, 21).

A mouse knock-out of NDPK-A and a double knock-out of NDPK-A and B have previously been reported (2, 23–25). Surprisingly, *NDPK-A$^{-/-}$* (*nme1$^{-/-}$*) mice, with the exception of having reduced birth weight and delayed mammary development, are phenotypically normal (25). Conversely, the *NDPK-A* and -B double knock-outs (*NDPK-A$^{-/-}$/NDPK-B$^{-/-}$*, also known as *nme1$^{-/-}$/nme2$^{-/-}$* mice) are stunted in growth and die perinatally due to severe anemia and abnormal erythroid

[3] The abbreviations used are: NDPK, nucleoside diphosphate kinase; TCR, T cell receptor; TNP, trinitrophenyl; KLH, keyhole limpet hemocyanin.
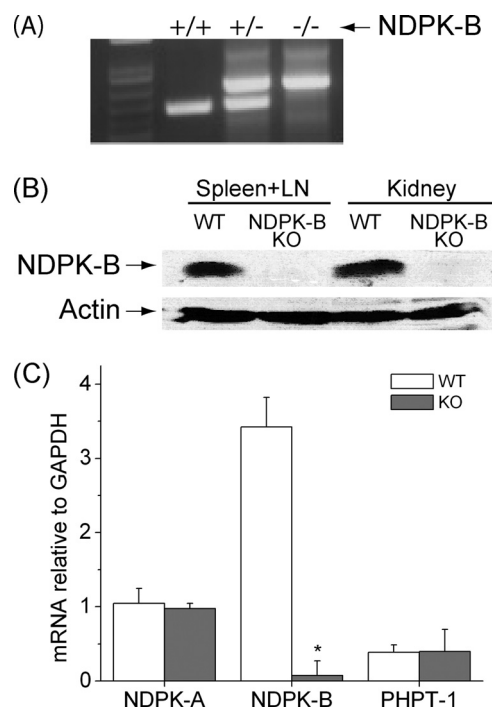
FIGURE 1. **Generation of *NDPK-B$^{-/-}$* mice.** *A*, to amplify the WT NDPK-B allele, oligonucleotides were synthesized that were complementary to genomic DNA on either side of the insertion site of pMS1 and used to amplify the WT locus by PCR. The mutant NDPK-B locus was amplified by PCR using the same 5′ oligonucleotide used to amplify the WT locus and an antisense 3′ oligonucleotide complementary to the 5′ end of pMS1. *B*, total lysates were isolated from kidneys and spleens of *NDPK*$^{-/-}$ and WT mice and Western-blotted with antibodies to NDPK-B. The same blot was then reprobed with antibodies to β-actin to demonstrate equal loading of protein in both lanes. *C*, expression of NDPK-B, NDPK-A, and PHPT-1 was determined by real-time PCR in Th1 cells isolated from WT and *NDPK*$^{-/-}$ mice. Shown is the relative amount of expression standardized to a GAPDH control ($n = 3$); $p < 0.001$ as compared with its WT. *LN*, lymph nodes; *KO*, knock-out.

development (23, 24). We generated *NDPK-B$^{-/-}$* mice to assess the specific role of NDPK-B in cellular development and function.

MATERIALS AND METHODS

Mice—The ES cell line (clone 69C10, strain 129/ola) containing an exon-trapping plasmid pMS1 integrated between exon 3 and exon 4 of the *NDPK-B* (*Nme2*) gene was purchased from the Center for Modeling Human Disease at University of Toronto. ES cells (strain 129/ola) were injected into C57BL/6 blastocysts at the transgenic facility at New York University Medical Center, and chimeric mice were obtained. *NDPK-B$^{+/-}$* mice were backcrossed eight generations with C57BL/6 and were then used to generate the *NDPK-B$^{-/-}$* C57BL/6 mice used in these studies.

The primers used to genotype mice were as follows: NDPK-B R(4957–4980), TCC CTA TAT ACC TGC TCT GCC TCA; NDPK-B F(4512–4535), CCT ATG TGG GAA ACA ATG GGT TTC; and pMS1 F, TTA GCA GCT CTG GAG CTT GCA GCC.

Cell Purification and Differentiation—CD4$^+$ T cells were purified on MACS beads (Miltenyi Biotech) from wild-type (WT) or NDPK-B$^{-/-}$ spleens, as described previously (26). Various CD4 T cell subsets were generated by culturing under Th1-polarizing conditions (100 units/ml IL-12 and anti-IL-4),
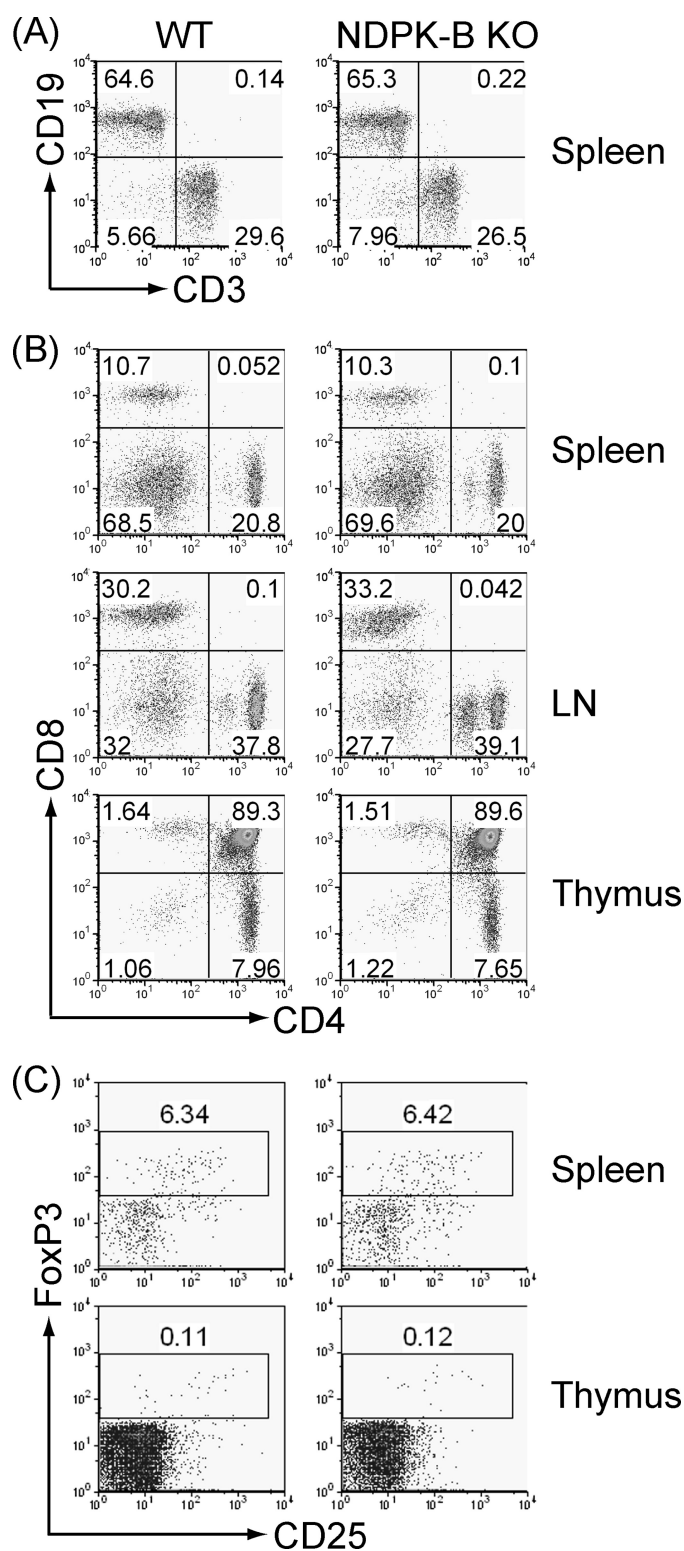

FIGURE 2. **T and B cell development is normal in *NDPK-B/nme2$^{-/-}$* mice.** Cells were isolated from spleen, thymus, and lymph nodes (*LN*) from WT and *NDPK-B$^{-/-}$* mice and stained with antibodies to CD3 and CD19 (*A*), CD4 and CD8 (*B*), or CD25 and FoxP3 (*C*), followed by FACS analysis. All experiments shown are representative of at least three experiments performed on cells isolated from at least three separate mice.

Th2-polarizing conditions (100 units/ml IL-4 and anti-IFN-γ), or Th17-polarizing conditions (2 ng/ml TGF-β, 20 ng/ml IL-6, anti-IL-4, and anti-IFN-γ) for 4–6 days.
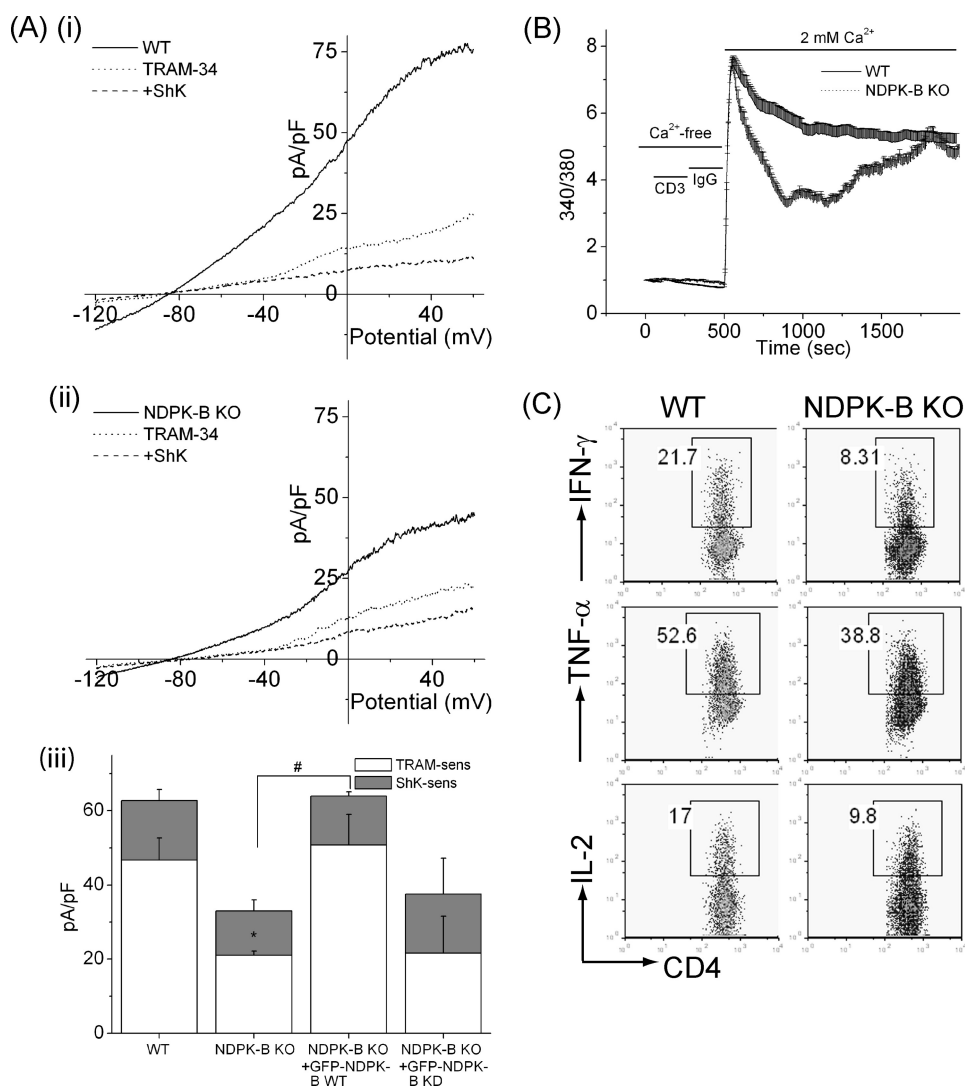
FIGURE 3. **Decreased KCa3.1 channel activity and TCR-stimulated Ca^{2+} flux and cytokine production in NDPK-B$^{-/-}$ CD4 Th0 cells.** *A, panels i and ii*, whole-cell patch-clamp experiments of CD4 T cells isolated from spleens of WT or *NDPK-B$^{-/-}$* mice following stimulation for 48 h with anti-CD3 and anti-CD28 antibodies; *panel iii*, bar graph summary at $+60$ mV of WT and NDPK-B$^{-/-}$ CD4 Th0 cells and NDPK-B$^{-/-}$ cells expressing GFP-WT NDPK-B or GFP-kinase-dead NDPK-B. Kinase-dead NDPK-B contains the substitution of asparagine for histidine at position 118 and has been reported previously (18). An average from $n = 10$ cells for each condition is shown. KCa3.1 current was measured as the TRAM-34 (1 μM)-inhibited current, and Kv current as the ShK (1 nM)-inhibited current (31, 32). *, $p < 0.05$ compared with TRAM-34-sensitive current from WT; #, $p < 0.05$ TRAM-34-sensitive current as indicated. *B*, cells in *A* were rested overnight, and after loading with fura-2/AM (5 μM), Ca^{2+} flux was determined after cross-linking with anti-CD3 antibodies, as described under "Materials and Methods." *C*, cells in *A* were rested overnight, and after stimulating with anti-CD3 and anti-CD28 antibodies for 4 h in the presence of brefeldin A, IL-2, IFN-γ, and TNFα production was determined by flow cytometry following intracytoplasmic staining with antibodies as indicated. All experiments shown are representative of at least three experiments performed on cells isolated from at least three separate mice. *pF*, picofarads; *KO*, knock-out.

Whole-cell Patch-clamp Experiments—Whole-cell patch-clamp experiments were performed on CD4 T cells as described previously (27), with some modifications (5).

Intracellular Ca^{2+} Activity—T cells were loaded with 5 μM fura-2/AM (Molecular Probes) in RPMI 1640 medium and 10% FBS for 30 min at 22–25°C. Cells were attached to a polylysine-coated coverslip for 20 min, and Ca^{2+} imaging was done with an IX81 epifluorescence microscope (Olympus) and OpenLab imaging software (Improvision). For single-cell analysis, 340/380 nm fura-2 emission ratios of >100 cells per experiment were analyzed. Background fluorescence obtained from regions containing no cells was digitally subtracted from each image. To compare the different groups, the 340/380 nm ratio was normalized to 1 by dividing the fluorescence values at different time points to the cellular fluorescence at time 0. Area under the curve was integrated to compare the percentage change in the calcium fluorescence. Experiments were done more than three times.

FACS Analysis and Intracellular Cytokine Staining—Cell suspensions were stimulated with anti-CD3 (5 μg/ml) and anti-CD28 (5 μg/ml) antibodies or phorbol-12-myristate-13-acetate (50 ng/ml) and ionomycin (500 ng/ml) for 4 h in the presence of brefeldin A (20 mg/ml). After stimulation, cells were stained with anti-CD4 antibodies, followed by fixation with a BD Biosciences Cytofix/Cytoperm^{TM} fixation/permeabilization solution kit, followed by staining with antibodies to IFN-γ, IL-2, or TNFα as indicated.

Immunization and ELISA—To measure the primary thymus-dependent immune response, mice were immunized intraperitoneally with trinitrophenyl-conjugated keyhole limpet hemocyanin (TNP-KLH) absorbed to aluminum hydroxide (20 μg of TNP-KLH in 200 μl of PBS) followed by a second immunization on day 14. Serum was isolated 21 days after the first immunization and assayed for TNP-specific antibodies by ELISA as described previously (28). For assessment of secondary immune response, mice were injected intraperitoneally 8 weeks after the primary immunization with TNP-KLH/aluminum hydroxide (20 μg in 200 μl of PBS), and KLH-specific antibodies were determined 7 days later.

RESULTS

NDPK-B$^{-/-}$ (nme2$^{-/-}$) Mice—The ES cell line purchased from the Center for Modeling Human Disease contains the exon-trapping plasmid pMS1 integrated between exon 3 and exon 4 of the *NDPK-B* gene (clone 69C10). *NDPK-B$^{+/-}$* and subsequently *NDPK-B$^{-/-}$* mice were obtained and confirmed by genotyping (Fig. 1*A*). Western blotting of lysates from kidney and spleen using a polyclonal antibody to NDPK-B confirmed the absence of the NDPK-B protein in *NDPK-B$^{-/-}$*
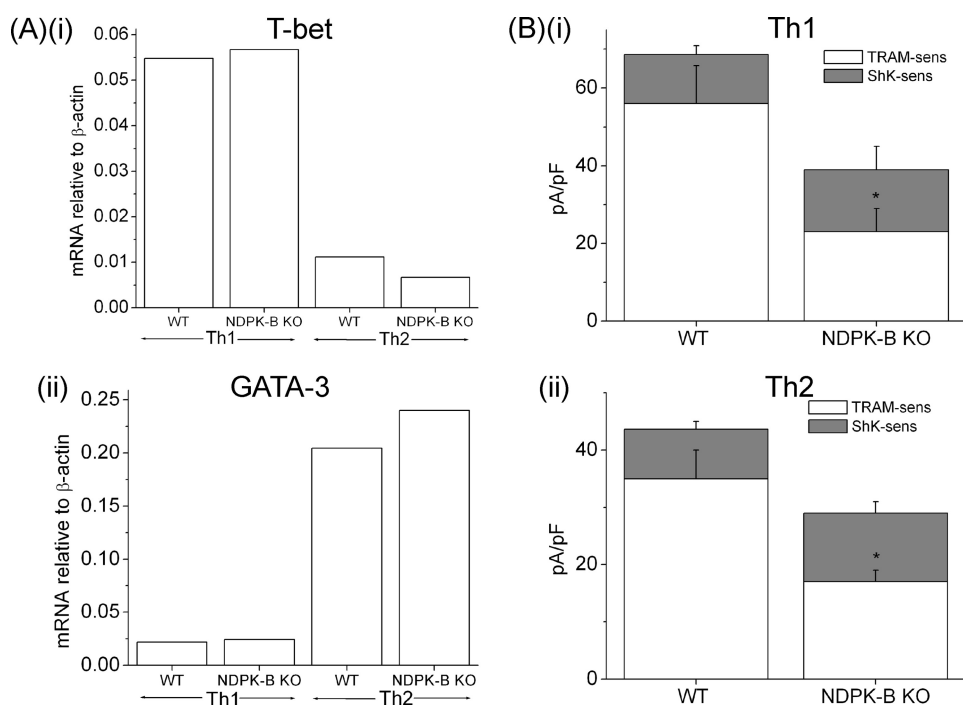
FIGURE 4. **Decreased KCa3.1 channel activity in NDPK-B$^{-/-}$ Th1 and Th2 cells.** *A*, real-time PCR of GATA-3 and T-bet expression in Th1- and Th2-differentiated cells. *B*, bar graph summary of whole-cell patch-clamp experiments performed on Th1 and Th2 cells using a protocol similar to that described for Fig. 2*A* (*n* = 10 cells). *, $p < 0.05$ compared with TRAM-34-sensitive current from the WT. *pF*, picofarads; *KO*, knock-out.

assessed 48 h after stimulation with anti-CD3 and anti-CD28 antibodies. As previously reported (30), KCa3.1 contributes to about two-thirds of the K$^+$ channel activity in Th0 CD4 T cells, whereas most of the remaining one-third of the K$^+$ channel activity is contributed by ShK-sensitive Kv channels, which are predominantly Kv1.3 and/or Kv1.1 or Kv1.6 (Fig. 3*A*, *panels i* and *iii*). KCa3.1 current was measured as the TRAM-34-inhibited current, and Kv current as the ShK-inhibited current. TRAM-34 and ShK have been shown to be specific inhibitors of KCa3.1 and the voltage-activated Kv channels, respectively (31, 32). Consistent with our previous findings that NDPK-B plays an important role in the activation of KCa3.1 (18), *NDPK-B$^{-/-}$* CD4 Th0 cells had about half of the KCa3.1 channel activity compared with WT cells (Fig. 3*A*, *panels i–iii*), confirming genetically that NDPK-B functions upstream of KCa3.1 activation. The finding that the expression of WT NDPK-B, and not kinase-dead NDPK-B, rescued KCa3.1 channel activity in *NDPK-B$^{-/-}$* Th0 cells (Fig. 3*A*, *panel iii*) indicates that the kinase activity of NDPK-B is required to activate KCa3.1. This is consistent with previous findings demonstrating that NDPK-B activates KCa3.1 by phosphorylating histidine 358 in the C terminus of KCa3.1 (18).

KCa3.1 channels play a critical role in Ca^{2+} influx by regulating membrane potential; the efflux of K$^+$ functions to maintain a hyperpolarized membrane potential, which functions to maintain a favorable electrochemical gradient to drive Ca^{2+} entry (5, 19, 29, 33). To address whether decreased KCa3.1 channel activity in *NDPK-B$^{-/-}$* CD4 Th0 cells leads to decreased Ca^{2+} influx, CD4 Th0 cells isolated from WT and *NDPK-B$^{-/-}$* mice were loaded with 5 μM fura-2/AM, and Ca^{2+} influx was assessed following stimulation with anti-CD3 antibodies. Stimulation of WT CD4 T cells with anti-CD3 antibody led to a marked increase in Ca^{2+} influx that was sustained for more than 30 min in WT CD4 Th0 cells (Fig. 3*B*). In contrast, although the initial rise in anti-CD3 antibody-stimulated Ca^{2+} influx was similar between WT and *NDPK-B$^{-/-}$* CD4 Th0 cells, Ca^{2+} influx rapidly decreased in *NDPK-B$^{-/-}$* Th0 cells, although over time it drifted back up toward the plateau phase of WT cells (Fig. 3*B*). Nevertheless, the calculated total Ca^{2+} influx, measured by integrating the area under the curve for 15 and 30 min, was significantly decreased by 30 ± 6.8% and 22 ± 5.2%, respectively, in *NDPK-B$^{-/-}$* CD4 Th0 cells compared with WT cells. Raw data were used to calculate the significance. The impairment in Ca^{2+} influx in *NDPK-B$^{-/-}$* CD4 Th0 cells was less than in *KCa3.1$^{-/-}$* cells (29), suggesting that the residual KCa3.1 channel activity in *NDPK-B$^{-/-}$* cells is sufficient to

mice (Fig. 1*B*). In the *NDPK-B$^{-/-}$* mice, exon 3 is spliced into pMS1, introducing a stop codon downstream of exon 3, leading to a truncated protein lacking exon 4, which contains the histidine kinase domain. This is unlikely to lead to a stable protein, because the NDPK-B protein was not detected in *NDPK-B$^{-/-}$* mice by Western blotting, and therefore the truncated mRNA was likely degraded by nonsense-mediated RNA decay. The absence of NDPK-B mRNA in *NDPK-B$^{-/-}$* mice was confirmed by real-time PCR (Fig. 1*C*). In addition, we did not detect changes in mRNA expression of NDPK-A or PHPT-1 (protein <u>h</u>istidine <u>p</u>hosphatase <u>1</u>) in *NDPK-B$^{-/-}$* mice that could compensate for the loss of NDPK-B (Fig. 1*C*); PHPT-1 has been shown to dephosphorylate several downstream targets of NDPK-B (Fig. 1*C*) (8).

T and B Cell Development in NDPK-B$^{-/-}$ Mice—NDPK-B$^{-/-}$ mice were born at the expected Mendelian frequency and were phenotypically normal. The total number of thymocytes and splenocytes was similar between WT and *NDPK-B$^{-/-}$* mice. In addition, T and B cell development were normal in *NDPK-B$^{-/-}$* mice. FACS analysis performed on spleen, lymph nodes, peripheral blood, and thymus demonstrated similar numbers of CD19$^+$ B cells (Fig. 2*A*), CD4$^+$ and CD8$^+$ T cells (Fig. 2*B*), and regulatory CD25 and FoxP3$^+$ regulatory CD4 T cells (Fig. 2*C*) in WT and *NDPK-B$^{-/-}$* mice.

Th0 Cells from NDPK-B$^{-/-}$ Mice Have Impaired KCa3.1 Channel Activity, TCR-stimulated Ca^{2+} Flux, and Cytokine Production—We have previously shown that KCa3.1 plays a critical role in Ca^{2+} influx and activation of Th0 cells (29). To assess whether NDPK-B is also important for activating Th0 CD4 T cells, CD4 T cells were isolated from the spleens of WT and *NDPK-B$^{-/-}$* mice, and KCa3.1 channel activity was
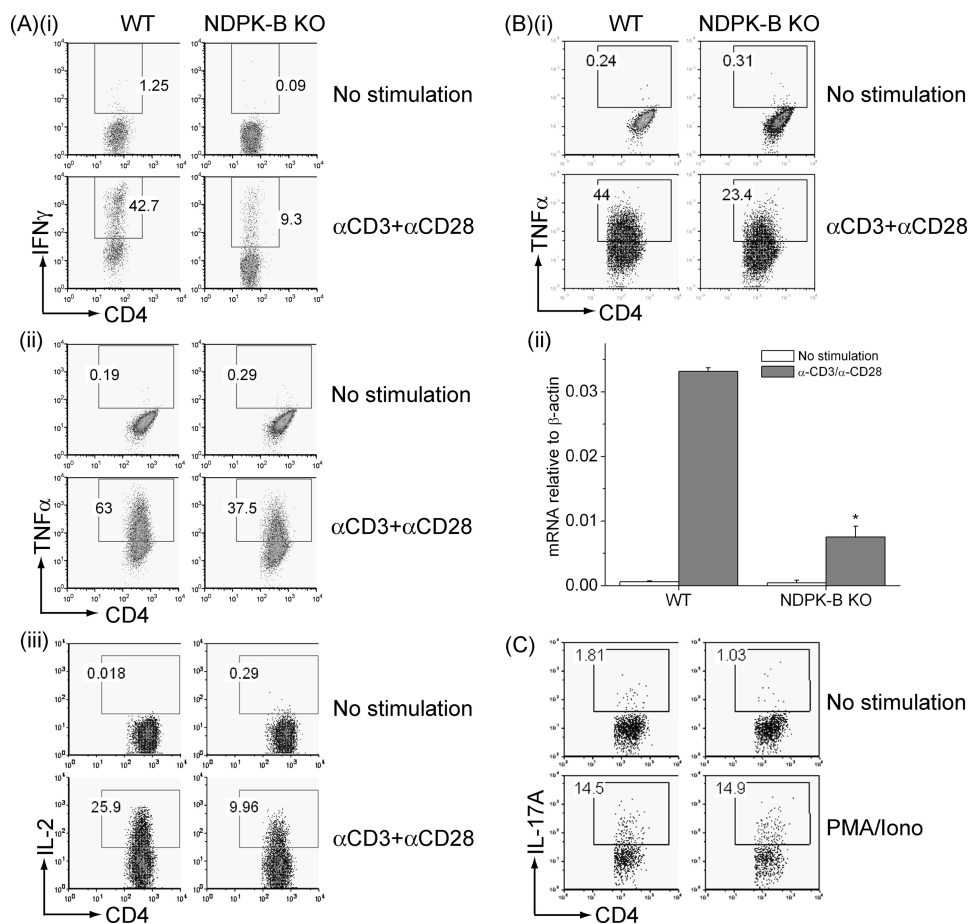
FIGURE 5. **Decreased TCR-stimulated cytokine production in NDPK-B$^{-/-}$ Th1 and Th2 cells.** *A*, Th1 cells were rested overnight, and after stimulating with anti-CD3 and anti-CD28 antibodies, IFN-γ (*panel i*), TNFα (*panel ii*), and IL-2 (*panel iii*) production was determined by flow cytometry as described for Fig. 2*C*. *B*, *panel i*, Th2 cells were rested overnight, and after stimulating with anti-CD3 and anti-CD28 antibodies, TNFα expression was assessed as described for Fig. 2*C*. *Panel ii*, IL-13 expression was determined by real-time PCR 4 h after stimulation with anti-CD3 and CD28 antibodies. Shown is the relative amount of IL-13 standardized to β-actin control. *, $p < 0.05$ as compared with WT stimulated cells. *C*, CD4 naive T cells were differentiated *in vitro* into Th17 cells, and IL-17 expression was assessed by intracellular staining after stimulation with phorbol-12-myristate-13-acetate and ionomycin. All experiments shown are representative of at least three experiments performed on cells isolated from at least three separate mice. *KO*, knock-out.

maintain a negative membrane potential during the plateau phase, when less Ca^{2+} is entering the cell.

A sustained increase in Ca^{2+} influx is required for the activation of NFAT-transcriptional complexes, leading to the induction of a number of cytokines required for T cell proliferation and survival. Anti-CD3/anti-CD28 antibody-stimulated IL-2, IFN-γ, and TNFα production was also decreased in NDPK-B$^{-/-}$ Th0 CD4 T cells (Fig. 3*C*), which is consistent with the defect in TCR-stimulated sustained Ca^{2+} influx.

NDPK$^{-/-}$ CD4 Th1 and Th2 Cells Have Decreased KCa3.1 Channel Activity and Are Defective in TCR-stimulated Ca^{2+} Flux and Cytokine Production, whereas Th17 Function Is Normal—We found that naive *NDPK-B$^{-/-}$* CD4 T cells differentiated normally into Th1 and Th2 when exposed to various culture conditions *in vitro*, as assessed by T-bet and GATA-3 expression using real-time PCR (Fig. 4*A*). Previous studies have demonstrated that Th1 and Th2 CD4 T cells resemble Th0 cells, with KCa3.1 contributing to about two-thirds of the K$^+$

channel activity and ShK-sensitive Kv channels contributing to the remaining one-third (30). In agreement with NDPK-B functioning upstream of KCa3.1 activation in Th1 and Th2 cells, KCa3.1 channel activity was markedly impaired in *NDPK-B$^{-/-}$* Th1 and Th2 cells, whereas in ShK-sensitive Kv channels was, if anything, slightly increased (Fig. 4*B*). Nevertheless, total K$^+$-channel activity was still decreased by more than 40% in NDPK-B$^{-/-}$ mice. In addition, the generation of IFN-γ, IL-2, and TNFα by *NDPK-B$^{-/-}$* Th1 cells (Fig. 5*A*) and that of IL-13 and TNFα by *NDPK-B$^{-/-}$* Th2 cells were impaired compared with WT cells (Fig. 5*B*). The production of TNFα was less impaired, possibly due to retained activation of the NF-κB pathway in knock-out cells. In contrast, Th17 function was normal in cells from *NDPK-B$^{-/-}$* mice (Fig. 5*C*), which is consistent with our previous finding that Th17 cells express predominantly ShK-sensitive Kv channels (29).

T Cell-dependent Antibody Production in NDPK-B$^{-/-}$ Mice—To assess whether NDPK-B is required to mount a normal response to immunization, WT and *NDPK-B$^{-/-}$* mice were vaccinated with the T cell-dependent antigen TNP-KLH, and the concentration of anti-hapten antibodies was determined by ELISA, as reported previously (28). The primary and secondary immune responses of mice immunized with TNP-KLH were similar between WT and *NDPK-B$^{-/-}$* mice, indicating that NDPK-B is not required to mount a normal, T cell-dependent antigen response (Fig. 6).

DISCUSSION

To identify the specific functions mediated by NDPK-B, we generated *NDPK-B$^{-/-}$* mice. In contrast to *NDPK-A$^{-/-}$/NDPK-B$^{-/-}$* double-knock-out mice, which are small at birth and die perinatally due to impaired erythroblast development (23, 24), *NDPK-B$^{-/-}$* mice are phenotypically normal, reproduce normally, and have a normal life span. This finding, coupled with a previous study demonstrating that *NDPK-A$^{-/-}$* mice have a mild phenotype (25), with the exception of being small at birth and having delayed mammary development, indicates that NDPK-A and -B perform a redundant role in erythroid development and perinatal survival. It has been proposed that the anemia and impaired erythroblast development in *NDPK-A$^{-/-}$/NDPK-B$^{-/-}$* mice may be accounted for by
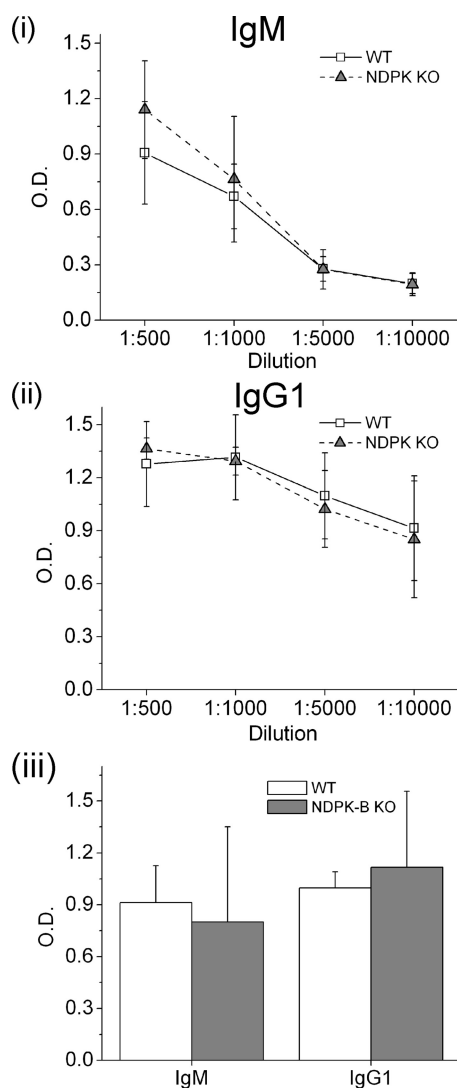
FIGURE 6. T cell-dependent antibody immune response is normal in *NDPK-B*$^{-/-}$ mice. Primary (*panels i* and *ii*) and secondary (*panel iii*) thymus-dependent immune responses were assessed by measuring TNP-specific IgM and IgG1 antibodies by ELISA as described under "Materials and Methods." *KO*, knock-out.

tive Kv channels and require Kv, not KCa3.1, channels for Ca^{2+} flux and Th17 production (29). We have now confirmed genetically that *NDPK-B*$^{-/-}$ mice mirror findings in *KCa3.1*$^{-/-}$ mice in that NDPK-B is required for full KCa3.1 channel activity and cytokine production in the same CD4 Th subsets in which KCa3.1 has been shown to function. Inhibition of KCa3.1 has been shown to be a good therapeutic target to treat murine models of autoimmune diseases mediated by Th1 cells (29) and to prevent the rejection of transplanted organs (34). Thus, these findings raise the possibility that specific pharmacological inhibitors of NDPK-B, if they could be developed, may be useful in treating similar conditions.

NDPK-B has also been proposed to play an important role in normal cardiac function and contractility, as well as to potentially contribute to pathologic remodeling in heart failure (6, 21, 22). *NDPK-B*$^{-/-}$ mice did not have any overt evidence of cardiac dysfunction until they reached 14 months of age. Future studies will definitively address whether *NDPK-B*$^{-/-}$ mice have subclinical changes in cardiac function and whether they are more susceptible to cardiac dysfunction in models of heart failure.

The *in vivo* relevance of the multiple enzymatic and biological functions assigned to NDPKs is still poorly defined. Thus, genetic evidence that NDPKs function to specifically regulate biological processes in physiologically relevant systems, such as knock-out animals, will be critical to identify the specific functions regulated by NDPKs and the biochemical mechanisms whereby NDPKs regulate these processes. Thus, the *NDPK-B*$^{-/-}$ mice described in this work will be an invaluable tool with which to uncover relevant physiological functions regulated by NDPK-B. Our finding that NDPK-B functions genetically upstream of KCa3.1 and is required for the activation of Th1 and Th2 cells, coupled with our previous studies demonstrating that NDPK-B activates KCa3.1 by phosphorylating His-318 in its C terminus (18), provides proof that NDPK-B functions *in vivo* to activate a subset of CD4 T cells and that its histidine kinase is important for this function.

REFERENCES

1. Desvignes, T., Pontarotti, P., Fauvel, C., and Bobe, J. (2009) *BMC Evol. Biol.* **9,** 256
2. Boissan, M., Dabernat, S., Peuchant, E., Schlattner, U., Lascu, I., and Lacombe, M. L. (2009) *Mol. Cell. Biochem.* **329,** 51–62
3. Mehta, A. and Orchard, S. (2009) *Mol. Cell. Biochem.* **329,** 3–15
4. Nallamothu, G., Dammai, V., and Hsu, T. (2009) *Mol. Cell. Biochem.* **329,** 35–44
5. Srivastava, S., Ko, K., Choudhury, P., Li, Z., Johnson, A. K., Nadkarni, V., Unutmaz, D., Coetzee, W. A., and Skolnik, E. Y. (2006) *Mol. Cell. Biol.* **26,** 5595–5602
6. Hippe, H. J., Lutz, S., Cuello, F., Knorr, K., Vogt, A., Jakobs, K. H., Wieland, T., and Niroomand, F. (2003) *J. Biol. Chem.* **278,** 7227–7233
7. Krishnan, K. S., Rikhy, R., Rao, S., Shivalkar, M., Mosko, M., Narayanan, R., Etter, P., Estes, P. S., and Ramaswami, M. (2001) *Neuron* **30,** 197–210
8. Klumpp, S. and Krieglstein, J. (2009) *Sci. Signal.* **2,** pe13
9. Lascu, I. and Gonin, P. (2000) *J. Bioenerg. Biomembr.* **32,** 237–246
10. Palacios, F., Schweitzer, J. K., Boshans, R. L. and D'Souza-Schorey, C. (2002) *Nat. Cell Biol.* **4,** 929–936
11. Murakami, M., Kaul, R., Kumar, P., and Robertson, E. S. (2009) *Mol. Cell. Biochem.* **329,** 131–139
12. Hartsough, M. T., Morrison, D. K., Salerno, M., Palmieri, D., Ouatas, T.,

decreased expression of the transferrin receptor (*Trf1* or CD71), resulting in reduced iron levels in erythroblasts (23, 24). Thus, these data suggest that both NDPK-A and -B perform a redundant function to regulate CD71 expression on the plasma membrane of erythroblasts.

NDPK-A and -B also perform non-redundant functions, and therefore the generation of specific knock-outs will be critical for identifying the biological functions that are specific to either NDPK-A or -B. For example, loss of NDPK-A alone was sufficient to inhibit the metastatic suppression of hepatocellular carcinoma (2, 25). We have previously shown that NDPK-B, but not NDPK-A, activates the K$^+$ channel KCa3.1 by phosphorylating histidine 358 in the C terminus of KCa3.1 (18). Previous studies of T cell function in *KCa3.1*$^{-/-}$ mice demonstrated that KCa3.1 is responsible for about two-thirds of K$^+$ channel activity in Th0, Th1, and Th2 cells and plays a critical role in TCR-stimulated Ca^{2+} influx and cytokine production by these cells (29). In contrast, Th17 cells contain predominantly ShK-sensi-

Mair, M., Patrick, J., and Steeg, P. S. (2002) *J. Biol. Chem.* **277,** 32389 –32399

13. Postel, E. H. (2003) *J. Bioenerg. Biomembr.* **35,** 31– 40
14. Kaetzel, D. M., Zhang, Q., Yang, M., McCorkle, J. R., Ma, D., and Craven, R. J. (2006) *J. Bioenerg. Biomembr.* **38,** 163–167
15. Lee, J. H., Marshall, J. C., Steeg, P. S., and Horak, C. E. (2009) *Mol. Cell. Biochem.* **329,** 141–148
16. Steeg, P. S., Bevilacqua, G., Kopper, L., Thorgeirsson, U. P., Talmadge, J. E., Liotta, L. A., and Sobel, M. E. (1988) *J. Natl. Cancer Inst.* **80,** 200 –204
17. Steeg, P. S. (2006) *Nat. Med.* **12,** 895– 904
18. Srivastava, S., Li, Z., Ko, K., Choudhury, P., Albaqumi, M., Johnson, A. K., Yan, Y., Backer, J. M., Unutmaz, D., Coetzee, W. A., and Skolnik, E. Y. (2006) *Mol. Cell* **24,** 665– 675
19. Cahalan, M. D. and Chandy, K. G. (2009) *Immunol. Rev.* **231,** 59 – 87
20. Chandy, K. G., Wulff, H., Beeton, C., Pennington, M., Gutman, G. A., and Cahalan, M. D. (2004) *Trends Pharmacol. Sci.* **25,** 280 –289
21. Hippe, H. J., Luedde, M., Lutz, S., Koehler, H., Eschenhagen, T., Frey, N., Katus, H. A., Wieland, T., and Niroomand, F. (2007) *Circ. Res.* **100,** 1191–1199
22. Hippe, H. J., Wolf, N. M., Abu-Taha, I., Mehringer, R., Just, S., Lutz, S., Niroomand, F., Postel, E. H., Katus, H. A., Rottbauer, W., and Wieland, T. (2009) *Proc. Natl. Acad. Sci. U. S. A.* **106,** 16269 –16274
23. Postel, E. H., Zou, X., Notterman, D. A., and La Perle, K. M. (2009) *Mol. Cell. Biochem.* **329,** 45–50
24. Postel, E. H., Wohlman, I., Zou, X., Juan, T., Sun, N., D'Agostin, D., Cuellar, M., Choi, T., Notterman, D. A., and La Perle, K. M. (2009) *Dev. Dyn.* **238,** 775–787
25. Arnaud-Dabernat, S., Bourbon, P. M., Dierich, A., Le Meur, M., and Daniel, J. Y. (2003) *J. Bioenerg. Biomembr.* **35,** 19 –30
26. Izcue, A., Hue, S., Buonocore, S., Arancibia-Cárcamo, C. V., Ahern, P. P., Iwakura, Y., Maloy, K. J., and Powrie, F. (2008) *Immunity* **28,** 559 –570
27. Wulff, H., Calabresi, P. A., Allie, R., Yun, S., Pennington, M., Beeton, C., and Chandy, K. G. (2003) *J. Clin. Invest.* **111,** 1703–1713
28. Fournier, E., Isakoff, S. J., Ko, K., Cardinale, C. J., Inghirami, G. G., Li, Z., Curotto de Lafaille, M. A., and Skolnik, E. Y. (2003) *Curr. Biol.* **13,** 1858 –1866
29. Di, L., Srivastava, S., Zhdanova, O., Ding, Y., Li, Z., Wulff, H., Lafaille, M., and Skolnik, E. Y. (2010) *Proc. Natl. Acad. Sci. U. S. A.* **107,** 1541–1546
30. Wulff, H., Miller, M. J., Hansel, W., Grissmer, S., Cahalan, M. D., and Chandy, K. G. (2000) *Proc. Natl. Acad. Sci. U. S. A.* **97,** 8151– 8156
31. Wulff, H., Castle, N. A., and Pardo, L. A. (2009) *Nat. Rev. Drug Discov.* **8,** 982–1001
32. Ghanshani, S., Wulff, H., Miller, M. J., Rohm, H., Neben, A., Gutman, G. A., Cahalan, M. D., and Chandy, K. G. (2000) *J. Biol. Chem.* **275,** 37137–37149
33. Grgic, I., Wulff, H., Eichler, I., Flothmann, C., Köhler, R., and Hoyer, J. (2009) *Transplant. Proc.* **41,** 2601–2606